ORIGINAL ARTICLE

SU2 Conference 2020, June 10-12, 2020

Implementation and validation of a new actuator disk model in SU2

E. Saetta[1*] | L. Russo[1†] | R. Tognaccini[1‡]

[1]Industrial Engineering Department, University of Naples Federico II, Naples, 80125, Italy

Correspondence
R. Tognaccini, Industrial Engineering Department, University of Naples Federico II, Naples, 80125, Italy
Email: rtogna@unina.it

Present address
Industrial Engineering Department, University of Naples Federico II, Piazzale Vincenzo Tecchio, 80, 80125, Naples, Italy

Funding information
Funds for the ordinary educational activity for university internal internships

The flow induced by rotary wings is an important topic in many fields and it is crucial in Aeronautics for the airframe integration. The simplest model adopted to simulate the effects of a rotary wing in the flow field is the actuator disk model which requires low computational cost in computational fluid-dynamics (CFD) analyses. Nowadays, many research programs all over the world are investigating the possibility to use distributed electric propulsion systems by propellers so that an advanced actuator disk model is fundamental for performance prediction by fast CFD analyses. A simple actuator disk model was implemented in the open source software *SU2* up to the release 7.0.6. In this paper a new and more general model, just implemented in *SU2*, is described; its application is discussed with different test cases and a procedure based on the optimal propeller theory for the automatic generation of the actuator disk input is provided.

KEYWORDS
Actuator Disk, propeller, SU2

[*]PhD student.
[†]Postdoctoral researcher.
[‡]Associate professor.

1 | INTRODUCTION

The actuator disk model was developed by *Rankine* and *Froude* [1] in the second half of the 19^{th} century. It allows, in a very simple manner, for the introduction in the flow of the velocity induced by a propeller of given thrust and power. To our knowledge its first applications in CFD date back to the late 80's. In particular, we recall the Euler flow simulations of a propfan configuration performed at Boeing [2] and a military turbo-prop aicraft analysis at NLR [3]. To date, all flow solvers, in practice, have an actuator disk model implemented and their applications ranges in all branches of Mechanic and Aerospace disciplines. Actuator disks can be inserted in numerical flow solvers as a *boundary condition* or adding *source terms* in the Navier-Stokes equations. The actuator disk model here presented is based on the first strategy.

The rising interest in the investigation of the *Distributed Electric Propulsion* (*DEP*) leads the actuator disk model to cover a fundamental position for the performance prediction by fast CFD analyses. By the way, the open-source CFD software *SU2* [4, 5] contained only a very simple actuator disk model up to the version 7.0.6. The need of a more powerful model in *SU2* has been felt for several reasons. First of all, we want to have the possibility to consider the presence of a propeller as accurately as possible at a low computational cost. However the model already implemented in *SU2* was too simplified because it assumed a uniform load along the disk radius and did not permitted to introduce the *swirl* in the flow. This is possible with the use of an actuator disk model which is based on the general momentum theory that will be discussed later. In addition, another drawback of the already implemented model is the required temperture jump, quite difficult to determine a-priori. The new model requires, as input, data that are typically known by the propeller designer such as thrust and power distribution along propeller radius.

The actuator disk models the propeller as a discontinuity surface through which a jump in the static pressure and in the velocity component tangential to the disk plane are imposed. Moreover, due to the mass conservation, the product between the fluid density ρ and the velocity component normal to the disk V_n is continuous across the disk:

$$(\rho V_n)_1 = (\rho V_n)_2 \tag{1}$$

where the subscripts 1 and 2 refer to the state 1 (upstream) and to the state 2 (downstream). The described variable

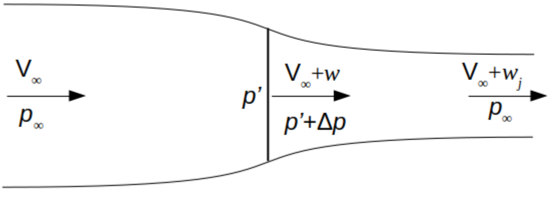

FIGURE 1 Actuator disk schematization in incompressible flow.

variations are predicted by the well known Momentum Theory which can be named Simple Momentum Theory, when only a constant pressure jump (Δp) along the propeller radius is imposed, or the General Momentum Theory, when the static pressure jump varies along the disk radius and the *swirl* term (the jump in the tangential velocity) is also included.

As shown in figure 1, in the case of incompressible flow, the Simple Momentum Theory, the axial velocity variation at the disk w is related to the one infinitely downstream by:

$$w = \frac{1}{2} w_j \tag{2}$$

According to [1], the total thrust T and total power P are respectively:

$$T = 2\rho A \left(V_\infty + w\right) w \tag{3}$$

$$P = T \left(V_\infty + w\right) \tag{4}$$

where A is the actuator disk area and V_∞ is the freestream velocity.

Using the equations (3) and (4), it is possible to compute the efficiency η:

$$\eta = \frac{T V_\infty}{P} \tag{5}$$

Two fundamental parameters of the Momentum Theories are the so-called *axial* and *rotational interference factors*, respectively:

$$a = \frac{w}{V_\infty}\,, \qquad a' = \frac{\omega}{2\Omega} \tag{6}$$

where ω is the angular velocity and Ω is the propeller angular velocity.

The differential form of the general momentum theory allows for a variable distribution along disk radius of axial and rotational inductions. The differential form of the associated thrust $\mathrm{d}T$, torque $\mathrm{d}Q$ and power $\mathrm{d}P$ are:

$$\mathrm{d}T = 4\pi\rho V_\infty^2 \left(1 + a\right) a r \mathrm{d}r \tag{7}$$

$$\mathrm{d}Q = 4\pi\rho V_\infty \Omega \left(1 + a\right) a' r^3 \mathrm{d}r \tag{8}$$

$$\mathrm{d}P = 4\pi\rho \left[V_\infty^3 \left(1 + a\right)^2 a r \mathrm{d}r + \Omega^2 V_\infty \left(1 + a\right) a'^2 r^3 \mathrm{d}r\right] \tag{9}$$

$$\mathrm{d}P = \Omega \mathrm{d}Q \tag{10}$$

In order to implement the actuator disk model as a *boundary condition* in a CFD code, it is necessary to face with the consistency and stability problem of the boundary conditions at the interface [6, p. 579]. For non linear problems, only theorems providing necessary conditions for the stability at the boundary exist, so the guideline to adopt in these cases is to be consistent with the *1D* characteristics theory. Considering the figure 2, the actuator disk is can be seen as an interface surface, the **State 1** is the state at upstream while the **State 2** is the state at downstream. The state on the disk is discontinuous according to the momentum theory.

According to the figure 2, for a subsonic inviscid flow these relations are respected:

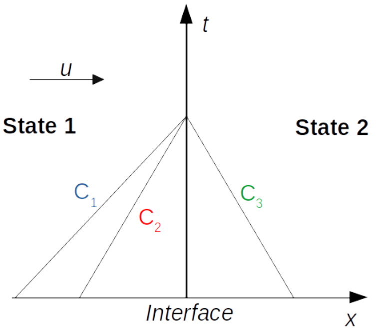

FIGURE 2 Characteristics curves at an interface for *1D* problems.

- C_1: R^+= constant along $\frac{dx}{dt} = u + c$
- C_2: s= constant along $\frac{dx}{dt} = u$
- C_1: R^-= constant along $\frac{dx}{dt} = u - c$

where c is the speed of sound, s is the entropy and $R^{\pm} = u \pm \frac{2c}{\gamma - 1}$ are the acoustic Riemann invariants.
Considering a *1D* interface, 2 data are extrapolated form **State 1** and 1 data is extrapolated from **State 2**. In order to be consistent with this theory, for *3D* problems, 4 data are extrapolated form **State 1** and 1 data is extrapolated from **State 2**.

This theory is useful to understand the choices done for developing the new boundary condition for the actuator disk model in the following sections.

2 | OLD *SU2* ACTUATOR DISK MODEL

As already mentioned, *SU2* 7.0.6 contains a simple actuator disk model, based on the simple momentum theory with a constant static pressure jump across the disk and no *swirl*. Moreover, a static temperature jump may be required by the actuator disk input: information difficult to be a-priori determined.

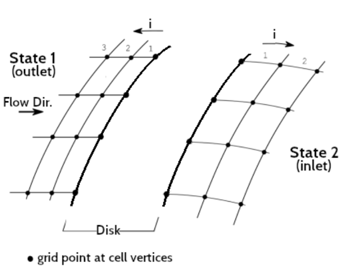

FIGURE 3 Scheme of a grid interface at actuator disk boundary condition for a generic node based solver.

Referring to figure 3, the following mathematical model can be defined upstream (State1) and downstream (State2) a disk interface in order to apply the Simple Momentum Theory:

State 1:

- 1 data imposed:
  - static pressure $p_1 = p_2 + \Delta p$
- 4 data extrapolated from upstream:
  - entropy s_1
  - acoustic Riemann invariant R_1^+
  - tangential velocity $\underline{V}_{t1}$

State 2:

- 4 data imposed:
  - static pressure jump Δp (constant)
  - static temperature jump ΔT
  - continuity $(\rho V_n)_2 = (\rho V_n)_1$
  - tangential velocity jump $\Delta V_t = 0$
- 1 data extrapolated from downstream:
  - acoustic Riemann invariant R_2^-

It can be notice that the characteristic theory is respected.

3 | NEW ACTUATOR DISK MODEL FOR *SU2* 7.0.7

The new actuator disk model implemented in *SU2* is based on the General Momentum Theory shortly described in section 1, details can be found in [7]. The hypothesis on which the model is based are the following:

- Inviscid compressible flow regime. The model is non-dissipative through the disk, but the it can be used for viscous simulations.
- Steady regime. The implemented boundary condition is steady, so the unsteady effects are neglected.
- Negligible angle between the disk axis and the freestream velocity. This implies that the model can simulate rotorcraft hovering (not tested), but it cannot be used for helicopter rotors in forward flight.

If the propeller convention is considered, the model can be used also for wind turbines, however it has not been tested yet.

The new model has been developed adding the following new functions in the *SU2* source code inside the class "CEulerSolver":

- "ReadActDisk_InputFile": this function reads the actuator disk data file given in input.
- "BC_ActDisk_VariableLoad": this function contains the local mathematical model for this new actuator disk model.

Moreover, other small *Set* and *Get* functions have been created and other functions modified.

This new model has been tested only for the compressible regime.

3.1 | Input

In order to generate the input file, the force coefficients have to be defined using the Renard relations:

$$C_T = \frac{T}{\rho_\infty n^2 D^4} \tag{11}$$

$$C_P = \frac{P}{\rho_\infty n^3 D^5} \tag{12}$$

$$C_R = \frac{F_R}{\rho_\infty n^2 D^4} \tag{13}$$

The advance ratio is defined as:

$$J = \frac{V_\infty}{nD} \tag{14}$$

Where n are rounds per second, D is the disk diameter and ρ_∞ is the freestream density. T, P and F_R are respectively the total thrust, total power and total radial force.

The user input for this new model is based on an external propeller data file. This file contains the propeller details in terms of thrust, power and radial force coefficient distributions along the disk radius. This kind of input has been chosen because, usually, the available data for a propeller are the performance in terms of load distribution. Moreover, in this way, the static temperature jump is no more required since it is computed by the model.

```
MARKER_ACTDISK= DISK DISK_BACK
CENTER= 0.0 0.0 0.0
AXIS= 1.0 0.0 0.0
RADIUS= 2.5146
ADV_RATIO= 2.81487
NROW= 37
# rs=r/R    dCT/drs     dCP/drs      dCR/drs
  0.2031   0.020066   0.0890674         0.0
  0.2235   0.019963   0.0932674         0.0
   ...       ...         ...            ...
  0.9591   0.434937   1.1470356         0.0
  0.9795   0.377288   0.9746048         0.0
```

FIGURE 4 Propeller data input file example for the new actuator disk model.

An example of the external propeller data file is reported in figure 4.

The propeller input file is composed by the following data:

- "MARKER_ACTDISK": actuator disk marker, the same used in the configuration file.
- "CENTER": actuator disk center coordinates.
- "AXIS": actuator disk axis unit vector pointing in the thrust direction.
- "RADIUS": actuator disk radius.
- "ADV_RATIO": actuator disk advance ratio.
- "NROW": the number of rows corresponding to the radial stations where the data are assigned.

The propeller performance are assigned using 4 columns:

- $\bar{r} = \frac{r}{R}$: non dimensional radial station.
- $\frac{dC_T}{d\bar{r}}$: local thrust coefficient per unit length.
- $\frac{dC_P}{d\bar{r}}$: local power coefficient per unit length.

- $\frac{\mathrm{d}C_R}{\mathrm{d}\bar{r}}$: local radial force coefficient per unit length.

Generally $\frac{\mathrm{d}C_R}{\mathrm{d}\bar{r}}$ is not known, so $\frac{\mathrm{d}C_R}{\mathrm{d}\bar{r}} = 0$ can be specified. As regards the configuration file, a new "ACTDISK_TYPE", named "VARIABLE_LOAD", has been introduced and a new option named "ACTDISK_FILENAME" has been added to specify the name of the propeller data file. If more actuator disks are considered, their data can be added at the end of the file.

3.2 | Relations between propeller performance and local variables

The local forces are introduced as source terms added to the diffusive flux on the cell faces. Considering the differential form of the aerodynamic force expression and using the advance ratio, it is possible to obtain the local axial force per unit area from equation (11):

$$F_a\left(\bar{r}\right) = \frac{2\rho_\infty V_\infty^2}{J^2 \pi \bar{r}} \left(\frac{\mathrm{d}C_T}{\mathrm{d}\bar{r}}\right) \tag{15}$$

F_a corresponds to the static pressure jump:

$$F_a\left(\bar{r}\right) = \Delta p\left(\bar{r}\right) \tag{16}$$

In the same way it is possible to compute the tangential force per unit area form equation (12) and the radial force per unit area from equation (13):

$$F_\theta\left(\bar{r}\right) = \frac{2\rho_\infty V_\infty^2}{\left(J \pi \bar{r}\right)^2} \left(\frac{\mathrm{d}C_P}{\mathrm{d}\bar{r}}\right) \tag{17}$$

$$F_R\left(\bar{r}\right) = \frac{2\rho_\infty V_\infty^2}{J^2 \pi \bar{r}} \left(\frac{\mathrm{d}C_R}{\mathrm{d}\bar{r}}\right) \tag{18}$$

According to the characteristics theory discussed in section 1, the local mathematical model for the new actuator disk model based on the General Momentum Theory is:

State 1:

- 1 data imposed:
  - static pressure $p_1 = p_2 + \Delta p$
- 4 data extrapolated from upstream:
  - entropy s_1
  - acoustic Riemann invariant R_1^+
  - tangential velocity $\underline{V}_{t1}$

State 2:

- 4 data imposed:
  - static pressure jump Δp (variable)
  - continuity $(\rho V_n)_2 = (\rho V_n)_1$
  - *swirl* $\Delta\left(\rho \underline{V}_t\right)$
- 1 data extrapolated from downstream:
  - acoustic Riemann invariant R_2^-

where the *swirl* term is given by the imposition of a momentum jump in tangential direction. It can be notice that the characteristic theory is respected.

4 | RESULTS

The new actuator disk model has been validated using two test cases provided by the Italian Aerospace Research Center (*CIRA*). The results obtained using *SU2* have been compared with those obtained by the *CIRA*'s *RANS* solver called *ZEN* [8]. For brevity, only the test case of an actuator disk with a semi-infinite spinner is reported in this paper[1]. For this test case the conditions are: $\alpha = 0^\circ$, $M_\infty = 0.56$, $Re_D = 36.5 \times 10^6$[2], considering an advance ratio of $J = 2.8$ and providing a thrust coefficient of $C_T = 0.18$. *RANS* equations with the *Spalart-Allmaras* turbulence model have been solved. The given input in terms of thrust and power coefficient distributions is reported in figure 5. The *Mesh*,

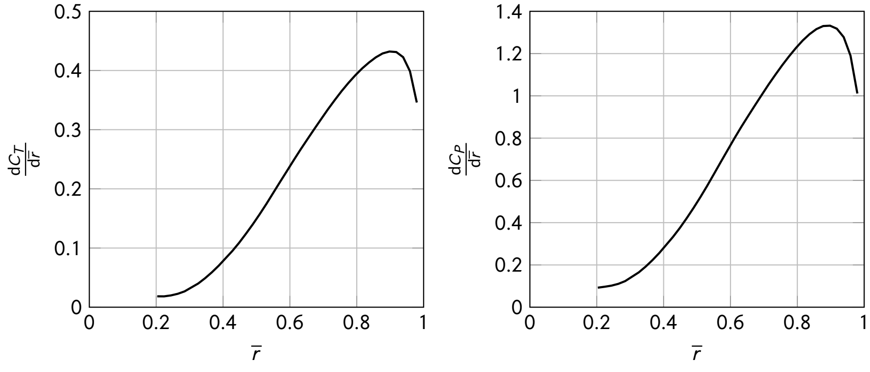

FIGURE 5 Thrust (left) and Power (right) coefficients distributions along the non-dimensional radius for the actuator disk with a semi-infinite spinner test case.

reported in figure 6, is built-up by 792576 cells. The comparison between *SU2* and *ZEN* results are reported in figures

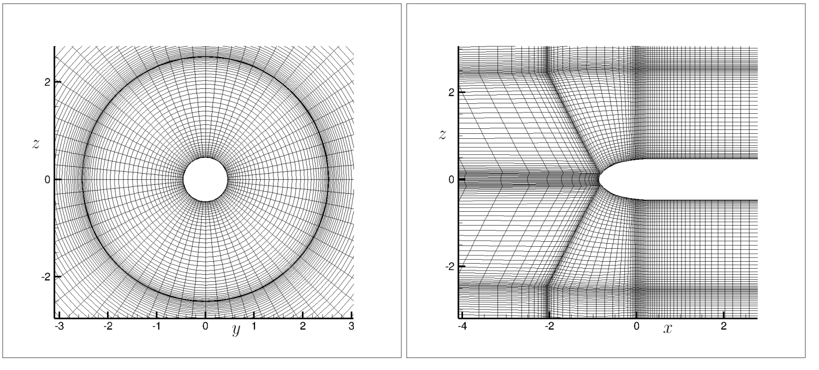

(a) (b)

FIGURE 6 *Mesh* details for the actuator disk with a semi-infinite spinner test case. Actuator disk (a) and spinner leading edge (b).

[1]This test case with a coarses grid has been included into *SU2* repository.

[2]The Reynolds number has been computed considering the actuator disk diameter for the Reynolds length.

7-10.

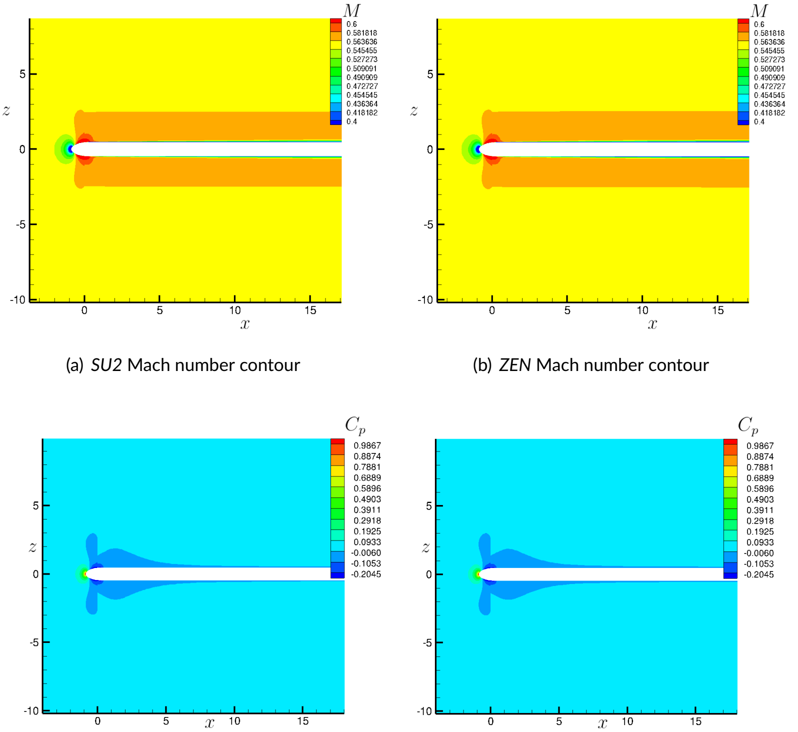

(a) *SU2* Mach number contour

(b) *ZEN* Mach number contour

(c) *SU2* C_p contour

(d) *ZEN* C_p contour

FIGURE 7 Mach number and pressure coefficient contours in axial plane obtained using *SU2* and *ZEN* for the actuator disk with semi-infinite spinner test case. $M_\infty = 0.56$, $Re_D = 36.5 \times 10^6$, $\alpha = 0°$.

The obtained results are in good agreement with those obtained by *CIRA* using *ZEN* and with the Momentum Theory predictions (downstream induction is twice the value on the disk and the *swirl* is zero upstream and constant downstream). Considering the figure 10 on the right, it is possible to notice that the static pressure is not equal to p_∞ in the streamtube due to the presence of the *swirl* term, leading to a possible conflict with the far field boundary condition.

The obtained results prove the validity of the new actuator disk model implemented in *SU2*. Two examples of application of present new model are proposed in the following.

The first application consists in a *DEP* configuration developed by *CIRA* reported in figure 11 at zero angle of attack with $M_\infty = 0.48$ and $Re_\infty = 16 \times 10^6$. *RANS* equations and *Spalart-Allmaras* turbulence model have been solved.

The obtained pressure coefficient contour is reported in figure 11 whereas, the cross flow at different distances in the wake of the tip propeller is reported in figure 12. It is evident that the introduction of the *swirl* term in the actuator disk model allows to capture the induced fluid rotation opposite to the tip vortex. The introduction of the *swirl* effect in the actuator disk model allowed the investigation of the reduction of the induced drag due to the presence of the tip propeller.

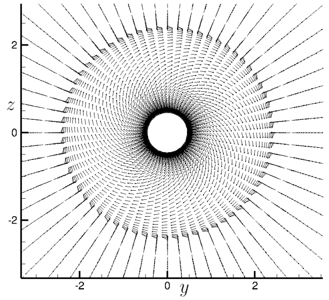

(a) *SU2*

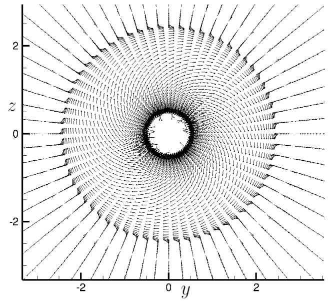

(b) *ZEN*

FIGURE 8 Tangential velocity vectors in the plane just behind the actuator disk. $M_\infty = 0.56$, $Re_D = 36.5 \times 10^6$, $\alpha = 0°$.

As regards the second application, it consists in a transoprt turboprop aircraft configuration at zero angle of attack considering $M_\infty = 0.50$ and $Re_\infty = 19 \times 10^6$. The propeller has an advance ratio of $J = 2.8$, providing a thrust coefficient of $C_T = 0.18$. The solved equations are the *RANS* using the *Spalart-Allmaras* turbulence model.

The *Mesh*, reported in figure 13(a), is composed by approximately 12 million of elements in half configuration. This means that for this case only half configuration has been considered due to limited computational resources. This implies that the propellers are counter-rotating, but generally the airplanes propellers are co-rotating.

In figure 13(b) the pressure coefficient contour on the surface of the aircraft is reported.

In figure 14, the pressure coefficient distributions along two wing sections within the actuator disk wake are reported. The propeller rotation produces a downwash and an upwash zone on the wing sections in the actuator disk wake, the difference between the red (downwash section) and the blue (upwash zone) curves show that there is a variation of the angle of attack due to the presence of the *swirl* term. It is possible to capture also this phenomenon with the new actuator disk model implemented in the version 7.0.7 of *SU2*. This is a typical problem of the airframe integration that is possible to appreciate also in *SU2* with this new model.

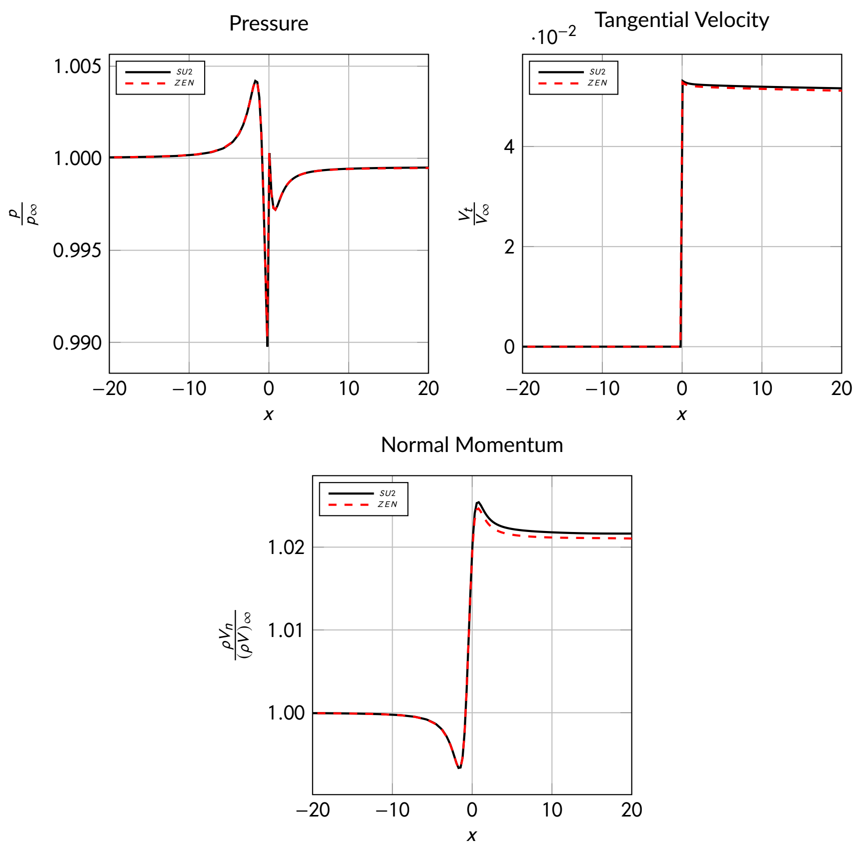

FIGURE 9 Distributions of flow properties in axial direction for $\overline{r} = 0.5$ for the actuator disk with a semi-infinite spinner test case. $M_\infty = 0.56$, $Re_D = 36.5 \times 10^6$, $\alpha = 0°$.

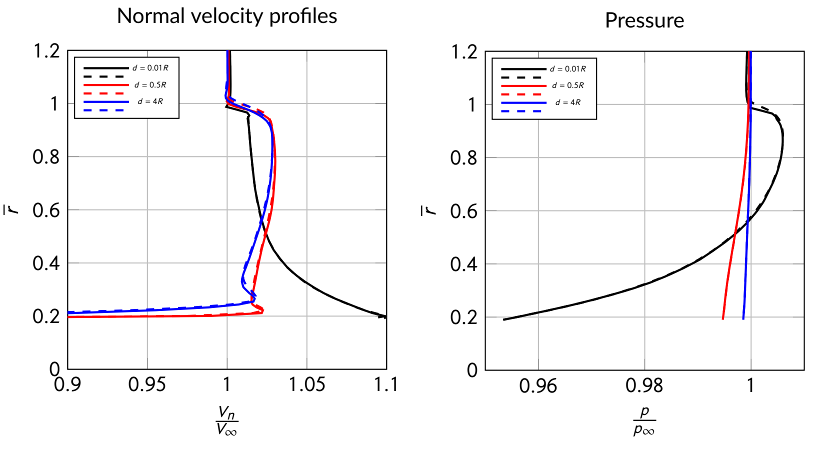

FIGURE 10 Distributions of non-dimensional flow properties in radial direction, for different distances d downstream the disk for the actuator disk with a semi-infinite spinner test case. $M_\infty = 0.56$, $Re_D = 36.5 \times 10^6$, $\alpha = 0°$. — : SU2; - - : ZEN

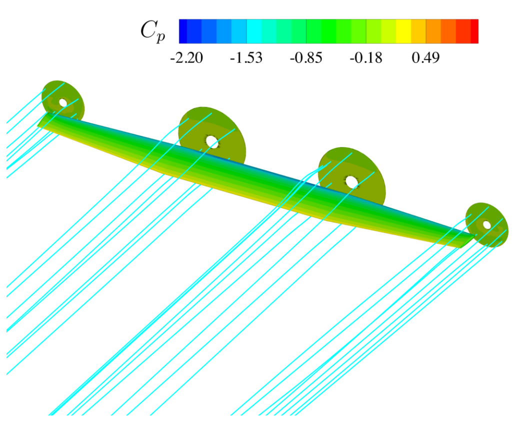

FIGURE 11 Pressure coefficient contour on the surface of the *DEP* configuration developed by *CIRA*. $M_\infty = 0.48$, $Re_\infty = 16 \times 10^6$, $\alpha = 0°$.

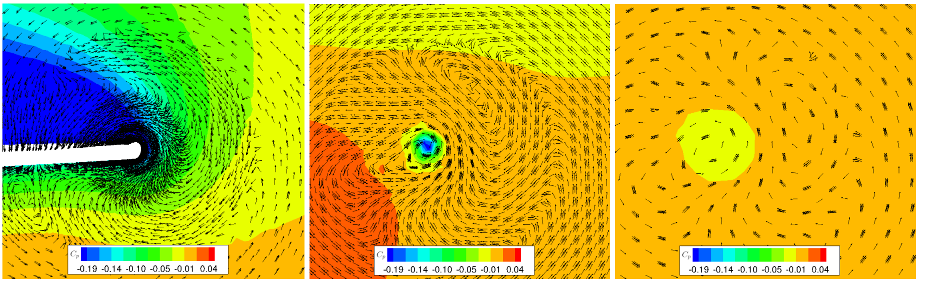

(a) $d = 1.5R$ (b) $d = 3R$ (c) $d = 5R$

FIGURE 12 Cross flow at different distances in the wake of the tip propeller for the *DEP* configuration developed by *CIRA*. $M_\infty = 0.48$, $Re_\infty = 16 \times 10^6$, $\alpha = 0°$.

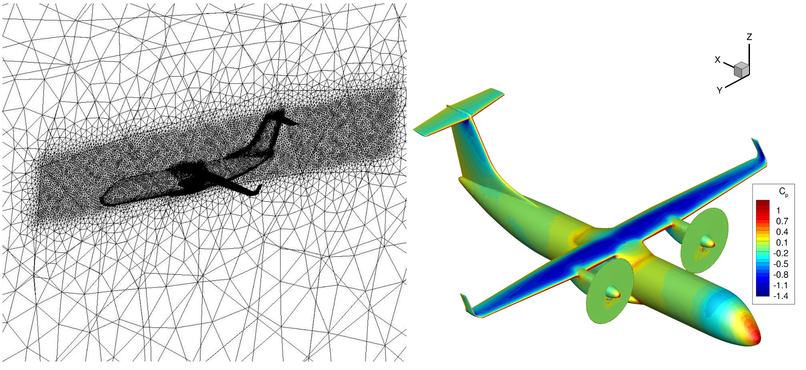

(a) (b)

FIGURE 13 (a) *Mesh* detail for the turboprop aircraft configuration. (b) Pressure coefficient contour on the aircraft surface. $M_\infty = 0.50$, $Re_\infty = 19 \times 10^6$, $\alpha = 0°$.

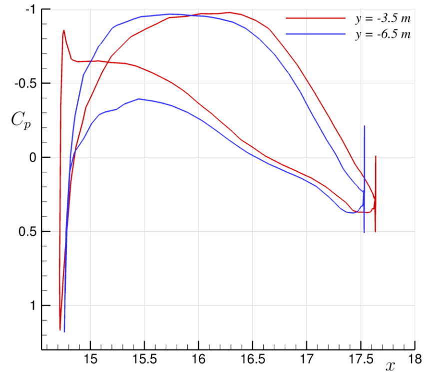

FIGURE 14 Pressure coefficient distributions along 2 wing sections in the propeller streamtube of the turboprop aircraft configuration. $M_\infty = 0.50$, $Re_\infty = 19 \times 10^6$, $\alpha = 0°$.
— downwash section; — upwash section.

5 | AUTOMATIC INPUT GENERATION FOR THE NEW ACTUATOR DISK MODEL

Very often, during aircraft preliminary design CFD analyses are required, but propeller details are not available. Generally the only known data are global parameters such as C_T, J and Ω. For this reason, it could be difficult to generate the input data file needed for the new actuator disk model implemented in *SU2*.

In order to overcome this problem, a *Python* script that provides the load distribution along the disk radius using global parameters has been developed. The script assumes that the adopted propeller is optimal, with the optimum interference factors $a\,(\bar{r})$ and $a'\,(\bar{r})$ [7]. An example of the optimal distributions of axial and rotational interference factors and the associated non-dimensional circulation are reported in figures 15 and 16.

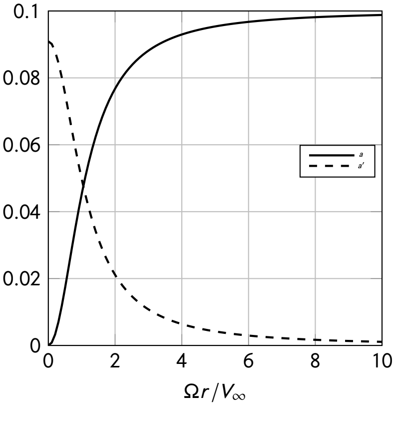

FIGURE 15 Axial and rotational interference factor distributions along the non-dimensional radius for the optimal propeller.

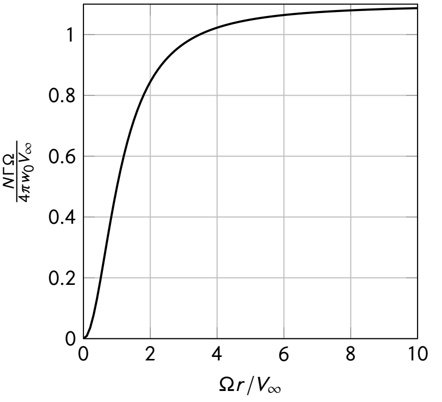

FIGURE 16 Non-dimensional circulation along the non-dimensional radius for the optimal propeller.

The *Python* script requires the following data by an interactive input assignment:

- Number of stations (corresponding to the "NROW" in subsection 3.1).
- C_T: thrust coefficient (based on the Renard definition).
- R: propeller radius.
- r_{hub}: radius of the propeller hub.
- J: advance ratio.
- V_∞: freestream velocity.
- N: number of propeller blades (required only if it is chosen to use the tip loss Prandtl correction function from equation (19)).

$$F(\overline{r}) = \frac{2}{\pi} arccos\left(e^{-\frac{N}{2}(1-\overline{r})\sqrt{1+\left(\frac{\Omega R}{V_\infty}\right)^2}} \right) \tag{19}$$

In order to obtain the optimal load distribution for the assigned C_T and J, the script adopts an iterative process using the false position method considering the error between the total C_T given in input and the one computed by integration of the thrust distribution obtained considering the axial interference factor distribution along the disk radius from the optimal propeller theory.

Once the process converges, the code provides a text file containing the propeller input data file to be given to *SU2*, and the plots of the load and the interference factors distributions.

It is possible to find this script in the *SU2* repository since the release 7.0.7.

6 | CONCLUSIONS

A new actuator disk model, based on the General Momentum Theory, has been developed and implemented in *SU2*. This model allows for adding a *swirl* term different from zero and a variable propeller load distribution to the simple model already implemented in the previous versions of the software.

The new model has been tested using two test cases provided by *CIRA*, and it has been successfully applied to a *DEP* configuration developed by *CIRA* and to a turboprop aircraft configuration. The results of the test cases are in agreement with the one obtained by another *RANS* solver named *ZEN* and developed at *CIRA*. The agreement with the momentum theory predictions strengthens the validity of the new model implemented in *SU2*. Moreover, the results of the two applications show the capability of *SU2* with this new actuator disk model to simulate the effects of propellers on the airframe.

Finally, a *Python* script providing an automatic generation of the propeller input data file has been developed in order to give the possibility to use the new actuator disk model even in case that the propeller load distribution is unknown.

References

[1] Betz A. Development of the inflow theory of the propeller; 1920.

[2] Yu N, Samant S, Rubbert P. Flow prediction for propfan configurations using Euler equations. AIAA paper 84-1645 1984;.

[3] Kassies A, Tognaccini R. Boundary Conditions for Euler Equations at Internal Block Faces of Multi-Block Domains Using Local Grid Refinement. AIAA Paper 90-1590 1990;.

[4] Palacios F, Colonno MR, Aranake AC, Campos A, Copeland SR, D ET, et al. Stanford University Unstructured (SU2): Anopen-source integrated computational environment formulti-physics simulation and design. 51st AIAA Aerospace Sciences Meeting including the New Horizons Forum and Aerospace Exposition 2013;.

[5] Economon TD, Palacios F, Copeland SR, Lukaczyk TW, Alonso JJ. SU2: An Open-Source Suite for Multiphysics Simulation and Design. AIAA Journal 2016;54(3):828–846.

[6] Hirsch C. Numerical Computation of Internal and External Flows, vol. 1. second ed. John Wiley & Sons, Ltd; 2007.

[7] Glauert H. Airplane Propellers. In: Aerodynamic Theory, vol. 4, W.F. Durand ed. Springer; 1935.p. 169–360.

[8] Marongiu C, Catalano P, Amato M, Iaccarino G. U-ZEN: A Computational Tool Solving U-Rans Equations for Industrial Unsteady Applications. 34th AIAA Fluid Dynamics Conference and Exhibit 2004-2345 2004;.